HHS Public Access

Author manuscript

Epilepsy Res. Author manuscript; available in PMC 2017 January 01.

Published in final edited form as:

Epilepsy Res. 2016 January ; 119: 30–33. doi:10.1016/j.eplepsyres.2015.11.006.

The pervasive reduction of GABA-mediated synaptic inhibition of principal neurons in the hippocampus during status epilepticus

Hua Yu Sun[a] and **Howard P Goodkin**[a,b,*]

[a]Department of Neurology, University of Virginia Health System, Charlottesville, VA 22908

[b]Department of Pediatrics, University of Virginia Health System, Charlottesville, VA 22908

Abstract

The goal of this study was to determine whether there are region-specific or time-dependent changes in GABA-mediated synaptic inhibition of principal neurons in the hippocampus during *in vivo* status epilepticus. Standard whole cell patch clamp electrophysiological techniques were used to characterize miniature inhibitory postsynaptic currents (mIPSCs) in recordings from the principal neurons (PNs) of the dentate gyrus, CA1, and CA3 in acutely-obtained hippocampal slices from control and lithium/pilocarpine-induced status epilepticus(SE)-treated animals. The reduction in mIPSC amplitude was pervasive across the 3 regions examined in hippocampal slices obtained after 60 minutes (late) or just 15 minutes after the onset of SE. The mIPSC frequency was reduced in all 3 regions after 60 minutes and 2 regions (dentate, CA1) after 15 minutes. These findings lend further support to the hypothesis that a rapid modification of the postsynaptic $GABA_A$ receptor population leads to a widespread decline in GABA-mediated inhibition that, in part, contributes to both the self-sustaining nature of SE and to the decrease in the efficacy of benzodiazepines.

Keywords

Status epilepticus; Pyramidal Neuron; dentate granule cell; $GABA_A$ receptors; miniature inhibitory postsynaptic currents

1. Introduction

Status epilepticus (SE) is a neurological emergency characterized by a prolonged, self-sustaining seizure that can result in death or neurological sequelae. There is general agreement that the genesis and maintenance of SE is, in part, the result of rapid

Department of Neurology, PO Box 800394, Charlottesville, VA, USA 22908. Tel.: (434) 924-5312, fax: (434) 982-1728, hpg9v@virginia.edu.

Disclosures

None of the authors has any relevant conflict of interest to disclose.

modifications in GABA-mediated inhibition that includes changes in the surface expression of the postsynaptic receptor population (Goodkin & Kapur, 2009).

The hippocampal CA3 region is activated and injured during SE (e.g. Motte et al., 1998). Although previous studies demonstrated changes in the characteristics of miniature inhibitory postsynaptic currents (mIPSCs) recorded from dentate granule cells (DGCs; Naylor et al., 2005; Goodkin et al., 2008) and CA1 Pyramidal Neurons (CA1 PyNs; Terenuma et al., 2008), no study has evaluated for changes in GABA-mediated synaptic inhibition of CA3 PyNs during *in vivo* SE.

Given the recent demonstration of region-specific, time-dependent differences in AMPA receptor-mediated currents during SE (Rajasekaran et al., 2012), we choose to confirm and extend the previous findings of the effect of SE on the characteristics of mIPSCs recorded from DGCs, CA1 PyNs, and CA3 PyNs in hippocampal slices acutely obtained from animals in SE induced using the combination of lithium and pilocarpine.

2. Methods

Male Sprague-Dawley rats postnatal day 15 to 25 were used. Animals were maintained with the dame. All animals were treated in accordance with the guidelines set by the University of Virginia Animal Care and Use Committee.

SE was induced via pretreatment with LiCl 3 mEq/Kg intraperitoneal followed 20 to 24 hours later by pilocarpine hydrochloride 50 mg/Kg intraperitoneal. After pilocarpine administration, animals were continuously monitored for behavioral seizures (SE-treated animals). Sixty (*late* SE) or 15 (*early SE*) minutes after the first observed Racine grade 5 seizure, the animals were anesthetized with isoflurane. Following decapitation, the brain was promptly removed for hippocampal slice preparation. Age-matched naïve animals (controls) were treated with saline. Coronal hippocampal slices (300 or 400 μm) were prepared using a vibrating microtome (VT1200S: Leica, Wetzlar, Germany) with the brain immersed in an ice-cold (1–3 °C) dissection buffer equilibrated with 95% O_2 – 5% CO_2. The dissection buffer was composed of the following (in mM): 120 NaCl, 3.5 KCl, 4.0 $MgCl_2$, 0.7 $CaCl_2$, 1.25 NaH_2PO_4, 26 $NaHCO_3$, and 10 glucose (300 mOsm). All chemicals were obtained from Sigma (St. Louis, MO). Slices were maintained for a minimum of 30 minutes at 30 °C prior to commencing electrophysiological recordings.

Whole cell patch clamp recordings of GABA-mediated mIPSCs in hippocampal slices and off-line analysis were performed using standard techniques as previously described (Goodkin et al., 2005; Goodkin et al., 2008). Superficial cells were avoided. All recordings commenced within 2 hours of hippocampal acute-slice preparation.

DGCs were visually identified as small- and medium-sized neurons with typical oval-shaped somas and a single process located within the dentate granule layer. PyNs were visually identified as cells with typical triangular shaped somas within the pyramidal layer.

Data is presented as means ± standard error (SEM). Error bars represent SEM. Statistical comparisons of the control, *early* SE-treated, and *late* SE-treated populations were

performed using a one-way ANOVA followed by a Holm-Sidak test (Prism v6.05, GraphPad Software, Inc).

3. Results

3.1 GABA-mediated synaptic inhibition of CA1 Pyns and DGCs was reduced after late SE

Recordings from CA1 PyNs and DGCs in acutely obtained control and *late SE*-treated slices confirmed previously published findings (Naylor et al., 2005; Goodkin et al., 2008; Terunuma et al. 2008) that mIPSC amplitude was reduced after *late SE* (Figs. 1–2; Fig. 3b, 3c). In these recordings, mIPSC frequency was also reduced. No changes were observed in rise time (date not shown) or decay (Fig. 1a).

3.2 GABA-mediated synaptic inhibition of CA3 PyNs was altered after late SE

Recording from CA3 PyNs in acutely obtained control and *late* SE-treated slices demonstrated that the reduction in GABA-mediated synaptic inhibition of principal neurons was pervasive within the hippocampus after *late* SE. In Fig. 2, traces recorded from a control CA3 PyN and *late* SE-treated CA3 PyN are displayed. The mIPSC frequency and median mIPSC amplitude for the control neuron was 0.41 Hz and 31.5 pA, respectively, compared to 0.13 Hz and 24.1 pA for the *late SE*-treated CA3 PyN. For the population of control CA3 PyNs (n = 9 cells, 6 animals), the mean of the median mIPSC amplitudes was 33.4 ± 2.8 pA. In comparison, the mean of the median mIPSC amplitudes for the *late SE*-treated CA3 PyNs (n= 9 cells, 7 animals) was 24.6 ± 1.9 pA ($p<0.05$; Fig. 2D). This ~25% decrease is similar to the reduction in recordings obtained from DGCs (29% decrease) and CA1 PyN (~35% decrease).

In addition to the decline in mIPSC amplitude, a decrease in mIPSC frequency (0.36 ± 0.09 Hz vs. 0.14 ± 0.02 Hz, $p<0.05$) was present (Fig. 2E). The rise time (data not shown) and decay (Fig. 2c′) were unchanged.

3.3 GABA-mediated synaptic inhibition was reduced after early SE

The reduction in GABA-mediated synaptic inhibition observed following the one hour SE time point in recordings from CA1 PyNs and DGCs, and now CA3 PyNs, has been posited to contribute to the pathogenesis of SE and benzodiazepine pharmacoresistance. As benzodiazepine pharmacoresistance is established rapidly after SE onset (Kapur & Macdonald, 1997; Jones et al, 2002; Goodkin et al, 2003), we chose to record mIPSCs from principal neurons in *early SE*-treated slices.

When compared to controls, both mIPSC frequency and amplitude were significantly decreased in recordings from DGCs in *early* SE-treated hippocampal slices. In Fig. 3A, averaged mIPSC traces from a control DGC and *early* SE-treated DGC are displayed. The mIPSC frequency and median amplitude for the control neuron was 0.33 Hz and 56.8 pA, respectively, compared to 0.13 Hz and 39.9 pA for the *early SE*-treated neuron. For the population of control DGCs (n = 9 cells, 5 animals), the mean mIPSC frequency was 0.28 ± 0.05 Hz and the mean of the median mIPSC amplitude was 51.3 ± 5.3 pA. In comparison, for the *early* SE-treated DGCs (n = 16 cells, 12 animals), the mean mIPSC frequency was

0.11 ± 0.02 Hz ($p < 0.05$) and the mean of the median mIPSC amplitude was 27.6 ± 2.5 pA ($p < 0.05$; Fig. 3B, 3C). The rise time (data not shown) and decay (Fig. 3a) were unchanged.

Recordings from the CA3 PyNs in the *early* SE-treated slices also demonstrated a decline in both mIPSC amplitude and frequency (Fig. 2d, 2e) compared to controls with no change in rise time or decay (data not shown). In the CA1 region, CA1 PyN mIPSC amplitude was reduced (Fig. 1b) but mIPSC frequency (Fig. 1c) was similar to controls in the *early* SE-treated slices as were rise time and decay (data not shown).

4. Discussion

SE is known to evolve through sequential clinical and electrographic phases (Lothman, 1990; Treiman et al., 1990). The region- and time-dependent cellular and molecular changes that support this electroclinical evolution are in the process of being unraveled (Naylor et al., 2005; Goodkin et al., 2008; Terunuma et al., 2008; Lugo et al., 2008; Rajasekaran et al., 2012; Naylor et al., 2013).

In this study, we confirmed those prior studies that demonstrated a modification in synaptic GABA-mediated inhibition of CA1 PyNs and DGCs after *late* SE (Goodkin & Kapur, 2009) and provide new evidence that this modification was pervasive and determined early in the course of SE. This early determination of a reduction in GABA-mediated synaptic inhibition lends further support to the hypothesis that this change may, in part, contribute to both the self-sustaining nature of SE and to the decrease in the efficacy of benzodiazepines.

Time-dependent changes in GABA-mediated synaptic inhibition of principal neurons at time points later than 60 minutes after the first Racine stage 5 seizure have not been investigated. Therefore, it is not known whether the changes in GABA-mediated synaptic inhibition as presented in this study persist during longer episodes of SE (e.g. super refractory SE). Rannals and Kapur (2011) observed an increase in the GABA-mediated synaptic inhibition of cultured hippocampal neurons as early as 12 hours after continuous exposure to a high potassium (7 mM KCl) external media that resulted in epileptiform bursting. Whether the homeostatic mechanisms responsible for that increase in GABA-mediated synaptic inhibition in culture are operative and would eventually lead to a further changes in the postsynaptic inhibitory response within the hippocampus during *in vivo* SE is not known.

Rajasekaran et al (2012) found that AMPA receptor-mediated currents recorded from CA1 PyNs in *late* SE were inwardly rectifying and philanthotoxin-sensitive. In addition, AMPA receptor-mediated currents recorded from DGCs at the late time point were neither inwardly rectifying nor philanthotoxin-sensitive. In contrast to the region- and time-specific changes for AMPA receptor-mediated transmission, a novel finding of this study is the demonstration that the reduction in GABA-mediated synaptic inhibition during both the early and late time points was pervasive across the principal neurons of the hippocampus consistent with a widespread modification of GABA-mediated synaptic inhibition of principal neurons during SE.

An important question to be addressed in a future study is whether these activity-dependent changes in inhibition and excitation are limited to the principal neurons or also effect

interneurons and the recruitment of inhibitory networks during SE (Pothmann et al, 2014). This further characterization of pre- and post-synaptic changes across the entire hippocampal network is necessary to better define the cellular mechanisms by which seizure termination fails and this dynamic, evolving neurological emergency persists.

Conclusion

This study (1) confirms prior studies demonstrating a modification in synaptic GABA-mediated inhibition of CA1 PyNs and DGCs after late SE, (2) provides additional evidence that this modification was determined early in the course of SE, and (3) extends the prior findings to synaptic inhibition of CA3 PyNs.

Acknowledgments

We thank Suchitra Joshi and Denise Grosenbaugh for their thorough review of this manuscript. This work was supported by NS067439 from the NINDS.

References

Goodkin HP, Liu X, Holmes GL. Diazepam terminates brief but not prolonged seizures in young, naïve rats. Epilepsia. 2003; 44:1109–12. [PubMed: 12887445]

Goodkin HP, Yeh JL, Kapur J. Status epilepticus increases the intracellular accumulation of $GABA_A$ receptors. J Neurosci. 2005; 25:5511–20. [PubMed: 15944379]

Goodkin HP, Joshi S, Mtchedlishvili Z, Brar J, Kapur J. Subunit-specific trafficking of $GABA_A$ receptors during status epilepticus. J Neurosci. 2008; 28:2527–38. [PubMed: 18322097]

Goodkin HP, Kapur J. The impact of diazepam's discovery on the treatment and understanding of status epilepticus. Epilepsia. 2009; 50:2011–8. [PubMed: 19674049]

Jones DM, Esmaeil N, Maren S, Macdonald RL. Characterization of pharmacoresistance to benzodiazepines in the rat Li-pilocarpine model of status epilepticus. Epilepsy Res. 2002; 50:3010–12.

Kapur J, Macdonald RL. Rapid seizure-induced reduction of benzodiazepine and Zn^{2+} sensitivity of hippocampal dentate granule cell $GABA_A$ receptors. J Neurosci. 1997; 17:7532–40. [PubMed: 9295398]

Lugo JN, Barnwell LF, Ren Y, Lee WL, Johnston LD, Kim R, Hrachovy RA, Sweat JD, Anderson AE. Altered phosphorylation and localization of the A-type channel, Kv4.2 in status epilepticus. J Neurochem. 2008; 106:1929–40. [PubMed: 18513371]

Lothman E. The biochemical basis and pathophysiology of status epilepticus. Neurology. 1990; 40(5 Suppl 2):13–23. [PubMed: 2185436]

Motte J, Fernandes MJ, Baram TZ, Nehlig A. Spatial and temporal evolution of neuronal activation, stress and injury in lithium-pilocarpine seizures in adult rats. Brain Res. 1998; 793:61–72. [PubMed: 9630518]

Naylor DE, Liu H, Wasterlain CG. Trafficking of $GABA_A$ receptors, loss of inhibition, and a mechanism for pharmacoresistance in status epilepticus. J Neurosci. 2005; 25:7724–33. [PubMed: 16120773]

Naylor DE, Liu H, Niquet J, Wasterlain CG. Rapid surface accumulation of NMDA receptors increases glutamatergic excitation during status epilepticus. Neurobiol Dis. 2013; 54:225–38. [PubMed: 23313318]

Pothmann L, Muller C, Averkin RG, Bellistri E, Miklitz C, Uebachs M, Remy S, Menendez de la Prida L, Beck H. Function of inhibitory micronetworks is spared by Na^+ channel-acting anticonvulsant drugs. J Neurosci. 2014; 34:9720–9735. [PubMed: 25031410]

Rajasekaran K, Todorovic M, Kapur J. Calcium-permeable AMPA receptors are expressed in a rodent model of status epilepticus. Ann Neurol. 2012; 72:91–102. [PubMed: 22829271]

Rannals MD, Kapur J. Homeostatic strengthening of inhibitory synapses is mediated by the accumulation of $GABA_A$ receptors. J Neurosci. 2011; 31:17701–12. [PubMed: 22131430]

Terunuma M, Xu J, Vithlani M, Sieghart W, Kittler J, Panagalos M, Haydon PG, Coulter DA, Moss SJ. Deficits in phosphorylation of $GABA_A$ receptors by intimately associated protein kinase C activity underlie compromised synaptic inhibition during status epilepticus. J Neurosci. 2008; 28:376–84. [PubMed: 18184780]

Treiman DM, Walton NY, Kendrick C. A progressive sequence of electroencephalographic changes during generalized convulsive status epilepticus. Epilepsy Res. 1990; 5:49–60. [PubMed: 2303022]

GABAergic synaptic inhibition of hippocampal PNs was diminished after late SE

Reduced synaptic inhibition of the PNs was determined early in the course of SE

Diminished inhibition of principal neurons was pervasive within the hippocampus

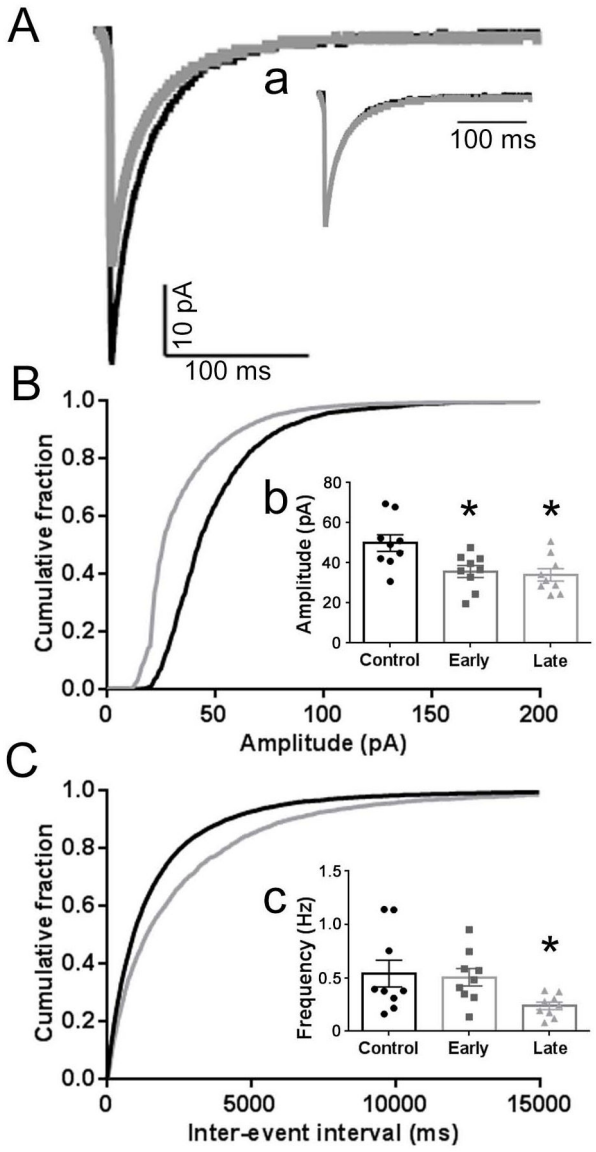

Fig. 1. Diminished GABAergic synaptic transmission in CA1 PyNs following SE

A, Averaged mIPSC traces from a control (black) CA1 PyN and a *late* SE-treated (gray) CA1 PyN voltage clamped to a holding potential of −60 mV. The mIPSC frequency, mean mIPSC amplitude, and median mIPSC amplitude for the control CA1 PyN was 0.38 Hz, 52.4 pA, and 47.6 pA, respectively, compared to 0.25 Hz, 38.8 pA, and 24.4 pA for the *late SE*-treated CA1 PyN. **a,** Normalized averaged mIPSC traces for the control and *late* SE-treated CA1 PyNs displayed in **A** demonstrating similar decays for these neurons (control 33 ms vs SE-treated 28 ms). The mean weighted decay for the population of *late* SE-treated CA1 PyNs (31.0 ± 0.6 ms) was similar to the controls (35.3 ± 2.9 ms; $p > 0.05$). **B, C**, Cumulative probability plots of mIPSC amplitude (**B**) and inter-event interval (**C**) obtained by pooling the data from 9 control CA1 PyNs from 6 animals (black) and 9 *late* SE-treated CA1 PyNs from 6 animals (grey). **b, c,** Inserted 3-bar bar graphs display the mean of the median mIPSC amplitudes (**b**) and mean mIPSC frequency (**c**) for the population of control

(black circles), *early* (gray squares; n = 9 from 6 animals) SE-treated CA1 PyNs, and *late* (gray triangles) SE-treated CA1 PyNs. For each inset, the median mIPSC amplitude and mean frequency for each individual neuron is represented by a single point. The mean of the median mIPSC amplitudes was 49.9 ± 4.2 pA for the control CA1 PyNs, 35.8 ± 3.0 pA for the early SE-treated CA1 PyNs, and 34.0 ± 3.1 pA for the *late* SE-treated CA1 PyNs. The mean mIPSC frequency was 0.54 ± 0.13 Hz for the control CA1 PyNs, 0.50 ± 0.10 Hz for the *early* SE-treated CA1 PyNs, and 0.24 ± 0.04 Hz for the *late* SE-treated CA1 PyNs. Compared to control population, the amplitude for the *early* and *late* SE-treated CA1 PyNs was reduced as was the frequency for the *late* SE-treated CA1 PyNs (*, $p < 0.05$).

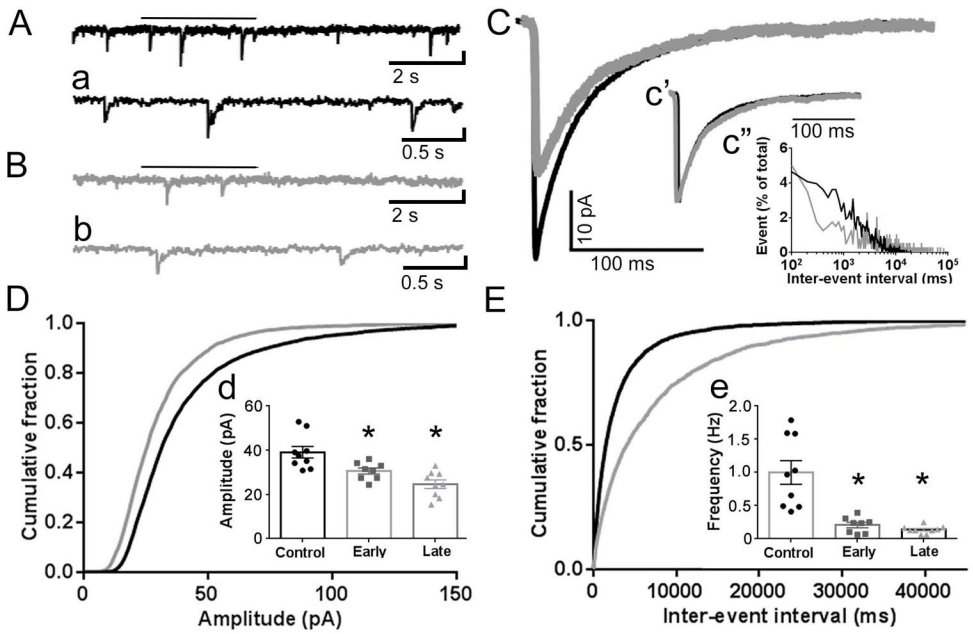

Fig. 2. Diminished GABAergic synaptic transmission in CA3 PyNs following SE

A, B, Representative current traces from a control CA3 PyN (**A**, black) and *late* SE-treated CA3 PyN (**B**, gray) voltage clamped to −60 mV. (**a, b,** expanded temporal resolution for traces displayed in **A, B**. The bar above each trace in **A** and **B** marks the segment displayed in **a** and **b**, respectively. **C,** Averaged mIPSC traces for the control (black) and *late* SE-treated neurons (gray) displayed in **A** and **B. c′**, Normalized averaged mIPSC traces for the control and SE-treated neurons displayed in A and B demonstrating similar decays for these neurons (control 20.03 ms vs. *late* SE-treated 22.15 ms). The mean weighted decay for the population of *late* SE-treated CA3 PyN (33.3 ± 3.6 ms) was similar to controls (27.4 ± 1.9 ms; $p > 0.05$). **c″**, Inter-event interval distribution for the control (black) and the *late* SE-treated (gray) neurons displayed in **A** and **B** demonstrating a prolonged inter-event interval and decrease in frequency for the *late* SE-treated neuron. **D, E,** Cumulative probability plots of mIPSC amplitude (**D**) and inter-event interval (**E**) obtained by pooling the data from the control and *late* SE-treated CA3 PyNs. **d, e,** Inserted 3-bar bar graphs display the mean of the median mIPSC amplitudes (**d**) and mean mIPSC frequency (**e**) for the populations of control (black circles), *early* SE-treated (gray squares; n = 8 from 6 animals) CA3 PyNs, and *late* SE-treated (gray triangles) CA3 PyNs. For each inset, the median mIPSC amplitude and mean frequency for each individual neuron is represented by a single point. The mean of the median mIPSC amplitude and mean mIPSC frequency for the control and *late* SE-treated CA3 PyN are provided in the text. For the early SE-treated CA3 PyNs, the mean of the median mIPSC amplitude was 30.59 ± 1.38 pA and the mean mIPSC frequency was 0.21 ± 0.04 Hz. Compared to controls, the amplitude and frequency for both the *early* and *late* SE-treated CA3 PyNs were reduced (* = $p < 0.05$).

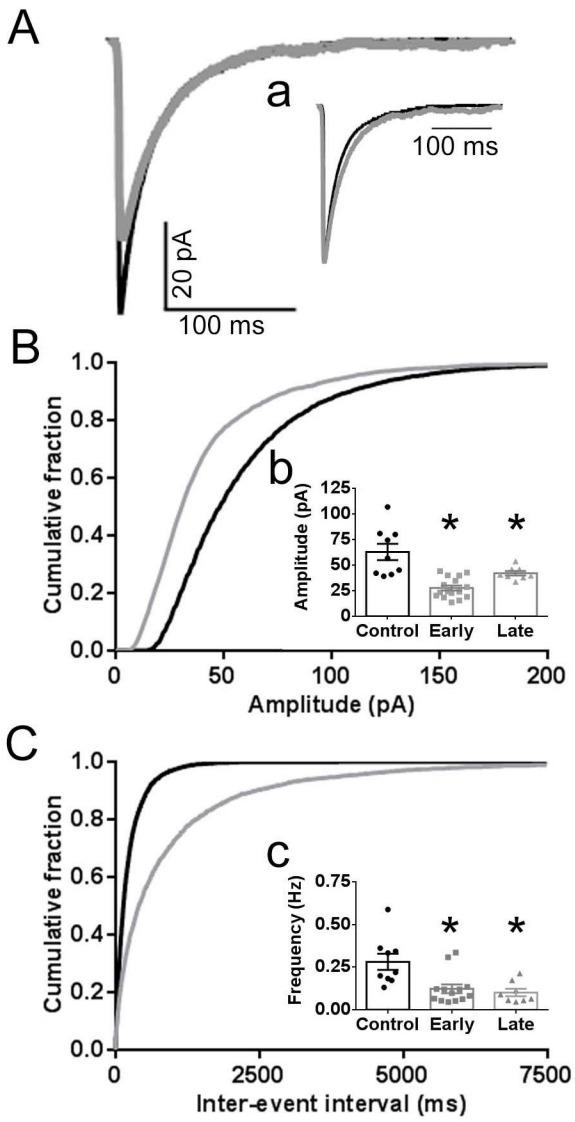

Fig. 3. Diminished GABAergic synaptic transmission in DGC following SE

A, Averaged mIPSC traces from a control (black) DGC and *early* SE-treated (gray) DGC voltage clamped to −60 mV. **a,** Normalized averaged mIPSC traces for the control and *early* SE-treated neurons displayed in **A** demonstrating similar decays for these DGCs (control 31 ms vs SE-treated 29 ms). The mean weighted decay for the populations of *early* (31.0 ± 1.8 ms) and *late* (30.9 ± 2.6 ms) SE-treated DGCs were similar to controls (30.7 ± 2.9 ms; $p > 0.05$). **B,C** Cumulative probability plots of amplitude (**B**) and inter-event interval (**C**) obtained by pooling the data from the control and *early* SE-treated DGCs. See text for further details. **b, c,** Inserted 3-bar bar graphs display the mean of the median mIPSC amplitudes (**b**) and the mean mIPSC frequency (**c**) for the populations of control (black circles), *early* SE-treated (gray squares) DGCs, and *late* SE-treated (gray triangles; n= 8 from 5 animals) DGCs. The median mIPSC amplitude and mean frequency for each individual neuron is represented by a single point. The mean of the median mIPSC amplitude and mean mIPSC frequency for the control and *early* SE-treated DGCs is

provided in the text. For the *late* SE-treated DGCs, the mean of the median mIPSC amplitude was 42.0 ± 2.2 pA and the mean mIPSC frequency was 0.10 ± 0.02 Hz. Compared to the control population, the amplitude and frequency for both the *early* and *late* SE-treated DGCs were reduced (* = $p < 0.05$).